VALIDATION OF FE MODEL FOR PREDICTING THE RESPONSE OF HEADED STUDS UNDER TENSION

VALIDIERUNG EINES FE-MODELLS FÜR DIE VORHERSAGE DES VERHALTENS VON KOPFBOLZEN UNTER ZUG

Johannes Holder, Hitesh Lakhani, Jan Hofmann

Institute of Construction Materials, University of Stuttgart

SUMMARY

In recent years, Finite Element analyses have gained more and more importance in the computation of the response of fasteners. Simulating concrete cone failure is numerically challenging due to the complex fracture process that should be captured, and known complexities associated with predicting fracture of concrete. In the present paper, validation of a numerical model developed in commercial Finite-Element software ANSYS® is presented. To validate the model, the study from Furche (1994) where the effect of head size on concrete cone break-out capacity was experimentally investigated, is simulated. Furthermore, the simulation results from the present study are also shown to compare well with other experimental and numerical results available in literature.

ZUSAMMENFASSUNG

In den vergangenen Jahren gewannen Finite-Elemente-Analysen in der Berechnung des Verhaltens von Verankerungen stetig an Bedeutung. Die numerische Simulation von kegelförmigem Betonausbruchs ist aufgrund des komplexen Bruchmechanismus und den bekannten Schwierigkeiten bei der Vorhersage von Betonversagen anspruchsvoll. In dieser Arbeit wird die Validierung eines numerischen Modells in der Finite-Elemente Software ANSYS® dargestellt. Für die Validierung des Modells wird die Arbeit von Furche (1994), in der der Einfluss der Kopfgröße auf das Versagen bei kegelförmigem Betonausbruch experimentell untersucht wurde, simuliert. Die Ergebnisse dieser Arbeit zeigen auch eine gute Übereinstimmung zu den Ergebnissen weiterer experimenteller und numerischer Untersuchungen aus der Literatur und validieren somit das Modell.

1. INTRODUCTION

Over the last decade the application of numerical simulation has grown massively in broad range of industrial sectors. The construction industry is no exception to this trend. Nowadays Finite-Element (FE) simulations play a crucial part not only for research but also in the design of structures. In the future, the influence of Finite-Element simulations will only increase. Further on at some time instance simulations may replace certain experiments and augment the necessary experimental investigations. The basic requirement for this to happen is development of capable simulation models that can reproduce material behaviour correctly under different stress states.

In fastening technology for many applications, the load carrying capacity of the fastener is limited by the base material which is concrete in the present study. This failure of the concrete for an anchor loaded in tension is referred to as the concrete cone failure. Simulating concrete cone failure had always been a challenging task [1–4] due to the complex fracture mechanism associated with this failure mode. The problem also inherits the problems and complexities associated with predicting fracture of concrete namely, the size effect [5, 6], an objective definition of tension behaviour of concrete [7] and numerical problems associated with crack localisation [8–10].

In the presented study, headed studs embedded in concrete and away from edge are simulated. Since, for a given embedment depth and concrete strength the concrete break out capacity of headed stud is known to be dependent on the head size (diameter) [11, 12]. The validation is performed for anchors with different head diameter. The well documented experimental study performed by Furche (1994) [13] to investigate the effect of head size was chosen for the validation presented in this paper. Further details about the experimental series executed by Furche (1994) are discussed in Section 2.

The simulations are performed using general purpose finite element software ANSYS® Mechanical [14]. The non-linear behaviour of concrete is modelled using Drucker-Prager concrete model with Rankine's yield surface in tension. Since, the objective of the study was to validate the material model for concrete and assess its suitability for predicting concrete cone failure. The steel for headed stud is assumed to be linear elastic.

Furthermore, the simulation results from the present study are also compared with experimental results from Eligehausen et al. (1992) [15] (other than those selected for the validation) and simulation results from Ozbolt & Eligehausen (1990) [1] and Fornusek & Konvalinka (2012) [16] where the effect of head size on concrete cone was investigated.

2. EXPERIMENTAL STUDY BY FURCHE (1994)

To investigate the influence of the head size of headed studs on the concrete cone capacity, an experimental investigation was conducted by Furche (1994) [13]. In this work, headed studs with an embedment depth of 80 mm and five different diameters of head were tested under tension. The shaft diameter, head thickness and support distance were kept same for all the tests. The diameter of the head was varied between 13 mm and 20 mm. The geometrical data of the tested studs can be found in Table 1. The concrete strength had slight variations as the anchors were embedded in slabs from different batches of concrete. The compressive strength ($f_{c,200}$) measured on cubes with edge length of 200 mm was reported to vary between 28.7 MPa and 33.4 MPa.

The results of this study showed a strong dependency of the ultimate load on the head size. With increased head sizes, the ultimate loads also increased. The results are discussed in more detail in section 4 in comparison to the numerical results.

Table 1: Geometrical details of the headed studs tested by Furche (1994) [13]

Head diameter (d_h)	13 mm	14 mm	16 mm	18 mm	20 mm
Shaft diameter (d_S)	12 mm				
Head thickness (t_h)	10 mm				
Embedment depth (h_{ef})	80 mm				
Radius of support ring	350 mm				

3. DETAILS OF THE NUMERICAL MODEL

3.1 Finite Element Software ANSYS® and element type

The commercial, general purpose Finite Element (FE) Software ANSYS Mechanical® is used for the numerical investigations presented in this paper. Being a general-purpose FE software, Ansys offers a wide range of element formulations and material models suitable for different purposes and material types. Here, both steel and concrete volume geometries are discretised using 3D

tetrahedral solid element referred as SOLID185 in the Ansys element help manual [17].

The element type SOLID185 is a linear element, that has three spatial degrees of freedom for each node. The standard shape of this element is a hexahedron (eight-node element) and different shapes like prisms and tetrahedrons are created by element degradation. Hence, for the tetrahedral option used in this study, multiple nodes are defined on the same point making it basically a four-node tetrahedral element. It should also be acknowledged that the used tetrahedral option can lead to reduced accuracy and a finer mesh is required in areas with high stress-gradient to receive realistic results. The element is used with its non-layered option and a simplified enhanced strain element formulation for concrete (Automatically selected by the Ansys element technology selector).

3.2 Material model: Concrete

As for the element type Ansys material library offers a range of material models that can be used for modelling concrete. Two most often used material models are: 1) The Menetrey-William model which was used by Lakhani et al. (2022) [3] & Lakhani and Hofmann (2022) [4] for simulating the concrete cone failure of headed studs under different fire exposure and 2) Drucker-Prager model with Rankine's yield surface in tension which was used by Lakhani and Hofmann (2022) [18] for investigating the effect of spalling on concrete cone failure capacity. Both models had been found to be suitable for capturing the response of headed stud under tension load.

The Drucker-Prager concrete model with Rankine's yield surface in tension is used in this work. Detailed information can be found in the ANSYS® material reference documentation [19] but for the completeness of the paper for the readers important information is summarized below.

The Drucker-Prager model with single yield surface is often used for describing materials that exhibit a similar material response under tension and compression. Thus, to capture the different compression and tension response of concrete the Drucker-Prager model needs modification. These modifications can be either: a) defining a second Drucker-Prager yield surface as shown by the elliptic failure curve (f_{DPt} – Shown in a two-dimensional cut of the yield function) in Fig. 1 or b) defining a composite surface consisting of a Rankine tension failure surface

(f_R) and a Drucker-Prager surface in compression (f_{DPc}). Both modification options are shown in Fig. 1.

The simulation results presented in this paper are performed with second modification i.e., originally elliptic Drucker-Prager yield surface (f_{DPc}) in compression is cut off in the tensile part and replaced by the Rankine's Surface (f_R). This surface can be identified by the straight lines in the plot and has the value of the ultimate tensile strength R_t in first and second principle (σ_1 and σ_2) directions.

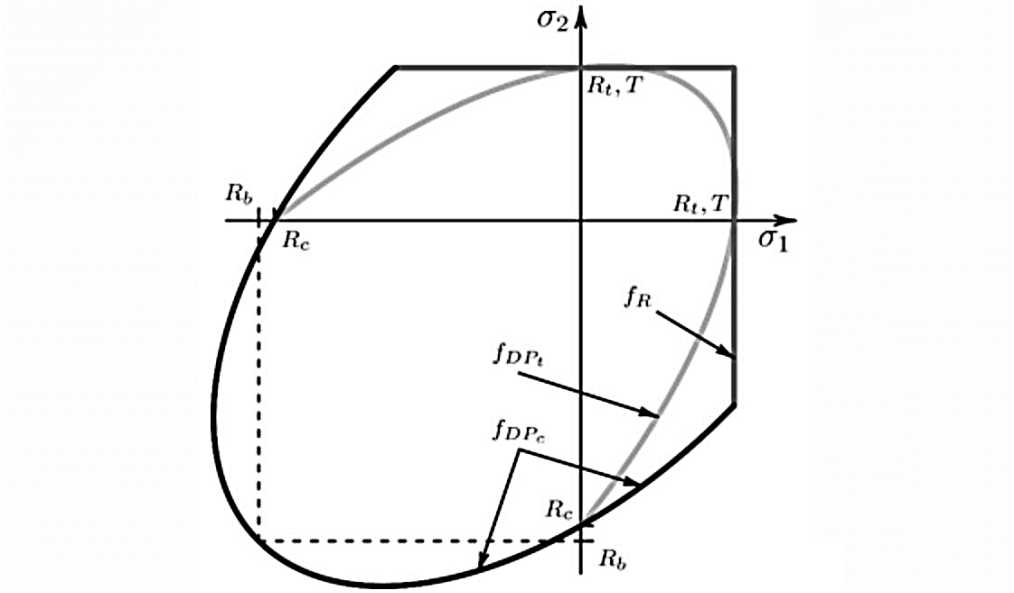

Fig. 1: Modified Drucker-Prager yield surfaces [19]

The hardening and softening behaviour of the yield surfaces are defined in terms of Ω_c and Ω_t, which are the hardening/softening function in compression and tension respectively, as shown in Fig. 2 (a) and (b). The hardening/softening function in compression (Ω_c) is defined using three nonlinear functions given by Equations 1 to 3 and in tension (Ω_t) is defined by Equation 4. In all the equations (1 to 4) κ is the hardening variable which is equal to the plastic strain component. Additionally, to help overcome mesh-dependent softening behaviour, the exponential softening for the tension yield function is normalized with an effective element length L_i.

The specific parameters for the hardening/softening functions for concrete that were used for the simulation results reported in this paper are given in Table 2. The parameters are based on the mean strengths and stress-strain constitutive law as per Eurocode 2 [20].

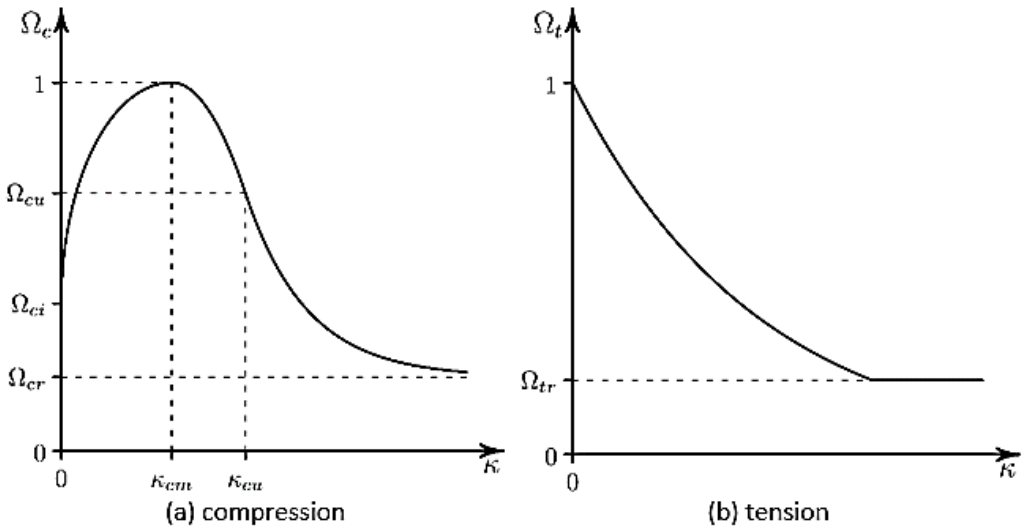

Fig. 2: Hardening/softening function in compression and tension for the exponential softening model [19]

The specific yield functions are:

- Compression, $\kappa < \kappa_{cm}$:

$$\Omega_c = \Omega_{ci} + (1 - \Omega_{ci}) \sqrt{2\frac{\kappa}{\kappa_{cm}} - \frac{\kappa^2}{\kappa_{cm}^2}} \tag{1}$$

- Compression, $\kappa_{cm} < \kappa < \kappa_{cu}$:

$$\Omega_c = 1 - (1 - \Omega_{cu}) \left(\frac{\kappa - \kappa_{cm}}{\kappa_{cu} - \kappa_{cm}}\right)^2 \tag{2}$$

- Compression $\kappa > \kappa_{cu}$:

$$\Omega_{cu} = \Omega_{cr} * (\Omega_{cu} - \Omega_{cr}) exp\left(2\frac{\Omega_{cu} - 1}{\kappa_{cu} - \kappa_{cm}} * \frac{\kappa - \kappa_{cu}}{\Omega_{cu} - \Omega_{cr}}\right) \tag{3}$$

- Tension:

$$\Omega_t = exp\left(-\frac{\kappa}{a_t}\right) \tag{4}$$

with: $a_t = \frac{g_{ft}}{R_t}$ and $g_{ft} = max\left(\frac{G_{ft}}{L_i}, \frac{R_t^2}{E}\right)$,
L_i is the effective element length, E is the Young's Modulus

Table 2: Material parameters for the concrete model

Symbol	Parameter name	Parameter
ρ_c	Density	2300 kg/m^3
E_c	Young's Modulus	29000 N/mm^2
ν_c	Poisson's Ratio	0.18
R_C	Uniaxial compressive strength	25.83 N/mm^2
R_t / T	Uniaxial tensile strength	1.9 N/mm^2
R_b	Biaxial compressive strength	29.70 N/mm^2
δ_t	Tensile dilatancy parameter	1
δ_c	Compression dilatancy parameter	1
κ_{cm}	Plastic strain at uniaxial compressive strength	0.0010093
κ_{cu}	Plastic strain at transition from power law to exponential softening	0.0021505
Ω_{ci}	Relative stress at start of nonlinear hardening	0.3
Ω_{cu}	Residual relative stress at κ_{cu}	0.8
Ω_{cr}	Residual compressive relative stress	0.2
G_{ft}	Mode I area-specific fracture energy	0.058N/mm
Ω_{tr}	Residual tensile relative stress	0.1

In the experiments from Furche (1994) [13], the target compressive strength ($f_{c,200}$ - tested with cubes of 200 mm edge length) for concrete was 30 MPa. As the mean compressive strength measured on a standard cylinder ($f_{cm,cyl}$) is used as input value for the model. The cylinder strength $f_{cm,cyl}$ = 25.83 MPa was obtained using conversion factors taken from Loch (2014) [21] ($f_{cm,cyl} = 0.82 \cdot 1.05 \cdot f_{cc.200}$).

3.3 Material models: Steel

In this work, all simulations are performed using linear-elastic steel model. The parameters used for the linear-elastic model are listed in Table 3.

Table 3: Material parameters of the linear-elastic steel model

Symbol	Parameter name	Parameter value
ρ_s	Density	7850 kg/m^3
E_s	Young's Modulus	200 000 N/mm^2
ν_s	Poisson's Ratio	0.3

3.4 Geometrical model and constraints

The test settings in the work of Furche (1994) [13], used large concrete slabs (3 m × 1 m × 0.25 m) with several studs casted into one slab. Since, experimentally the studs were spaced in a way that a full concrete cone breakout for each tested stud was guaranteed. Hence, for the numerical investigation the size of the slab is reduced to 1000 mm by 1000 mm by 250 mm. Since only one stud is simulated at a time, the chosen dimensions of the slab could be considered rather big for the embedment depth of 80 mm. But were needed for simulating the wide support ring with a radius of 350 mm.

Due to geometric symmetry, only a quarter of the actual geometry is modelled using two orthogonal symmetry conditions. In Fig. 3, the geometry and the constraints on the quarter model are shown. The headed stud is modelled as one body and has a frictionless contact with the concrete. The concrete slab is divided into three bodies which are connected as "Shared Topology" in ANSYS®. This means, that the bodies share the same nodes on the common surfaces. The concrete body in direct contact with the stud is 150 mm high and has a radius of 160 mm. The following concrete part is also 150 mm high and has an inner radius of 160 mm and an outer radius of 350 mm. The displacement is applied on the cross section of the headed stud's shaft which is projecting 50 mm above the concrete surface. The support condition is applied on an arc 350 mm from the headed stud's middle axis.

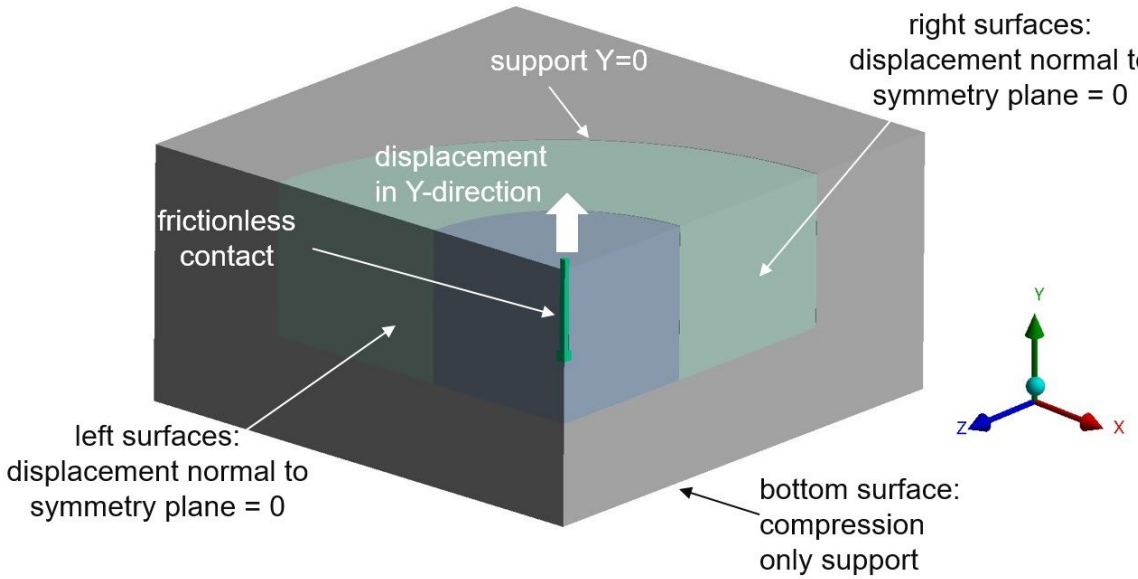

Fig. 3:Geometry and constraints of the models

3.5 Meshing

The reason for dividing the concrete slab into three parts is to have better control on the mesh sizes in different zones of the slabs. It should be noted that the approach adopted by the authors to control the meshing is not the only way to achieve the desired mesh. There are different options available in Ansys® which can be used by different users based on individual discretion. Near the headed stud where the concrete cone breakout will take place, the mesh size control parameter is selected to 10 mm element size and in the other concrete areas, an increased value is chosen to optimise the computation time. A very fine mesh is also applied on the headed stud and for the contact area between stud and concrete. An overview of the mesh sizes is shown in Fig. 4.

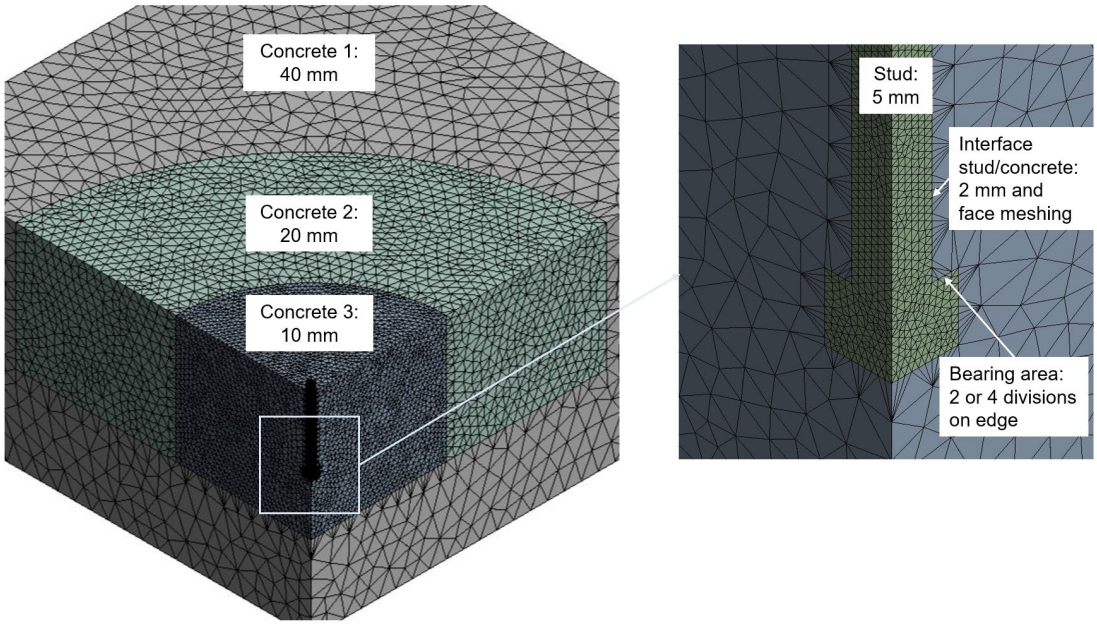

Fig. 4: Meshed view of the model

(2 divisions on the edge of the bearing area is used only for the head diameter 18 & 20 mm)

Since, the concrete cone breakout is expected to be limited to "Concrete 3" body, it has the smallest mesh size. The number of nodes & elements in "Concrete 3"-body for different models with head sizes are summarised in Table 4.

Table 4: Descsritisation details for "Concrete 3"-body

Head diameter [mm]	13	14	16	18	20
Number of nodes	38815	38924	39164	39057	39108
Number of elements	210927	211270	212302	211614	211945
Volume [mm^3]	3.01E+06	3.01E+06	3.01E+06	3.01E+06	3.01E+06
Average element size [mm]	4.27	4.26	4.25	4.26	4.26

4. RESULTS

As mentioned in section 2, Furche (1994) [13] observed a strong dependency between the ultimate loads and the head diameter of the studs. A similar behaviour was received in the numerical investigations. The experimental and simulation results as the variation of failure load with bearing area are shown in Fig. 5. The bearing area is the area on the top side of the stud's head over which the force is transmitted from the stud into the concrete. The experimental results (full dots in the figure) show that the ultimate load increases with increasing bearing area but the ultimate load seems to move towards an upper threshold. The development of the ultimate loads over different bearing areas is captured very well but the numerical results are all slightly lower than the experimental results. The results from the simulations are also listed in detail in Table 5.

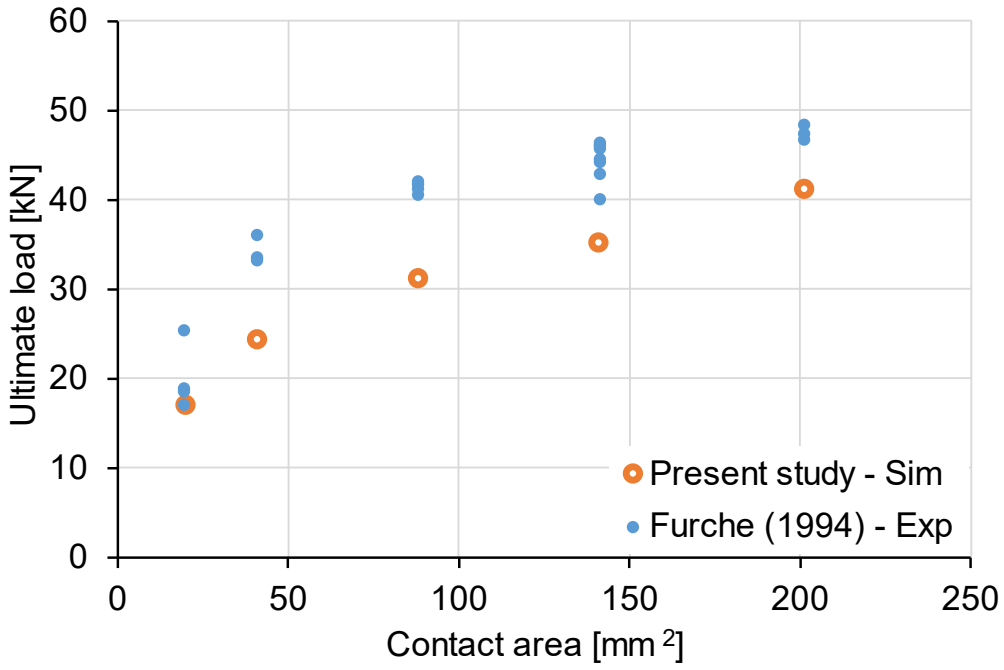

Fig. 5: Ultimate loads from the experiments and the simulations for different bearing areas

Table 5: Summary of the simulation results

Head diameter [mm]	13	14	16	18	20
Ultimate load - Simulation [kN]	17.07	24.35	31.17	35.18	41.21
Displacement at peak load - Simulation[mm]	1.62	2.36	1.62	1.44	1.36
Mean ultimate load - Experimental [kN]	19.92	34.06	41.36	44.49	47.5
Ratio (Ultimate load) Simulation/Experiment	0.86	0.71	0.75	0.79	0.87

The load-displacement curves for the simulations are shown in Fig. 6. The peak in the load-displacement curve becomes pronounced with increasing head diameter. The curves with a lower head diameter have a flatter curve in general and reach their ultimate load at a higher displacement.

The fracture patterns (based on principle tensile strain) for the simulation with 13 mm head size and 20 mm head size, are shown in Fig. 7 (a) and (b) respectively. These principle tensile strain contours are plotted at the point on the load-displacement curve where the load has passed the peak value and has reduced to 80% of the ultimate load.

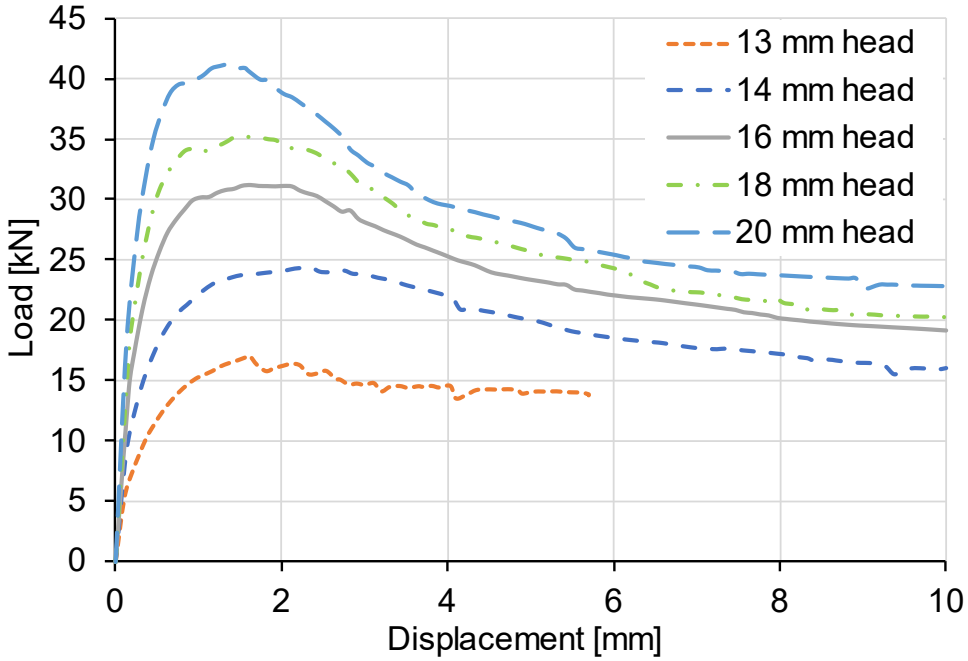

Fig. 6: Load-displacement curves for the simulations with linear-elastic steel model

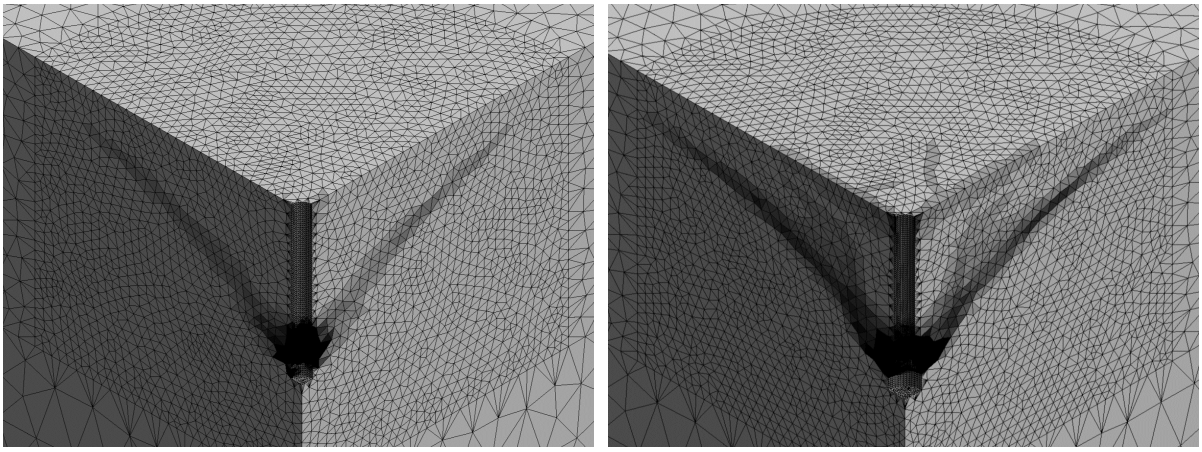

(a) 13 mm head *(b) 20 mm head*

Fig. 7: Fracture pattern (principle tensile strain contours) for different head sizes

The fracture patterns show another interesting difference between the simulations with different head diameter. In the pattern from the simulation with the smaller head, the fracture is much more local around the head of the stud, whereas for the 20 mm head diameter, the concrete cone breakout is much more clearly visible.

In early numerical investigations by Ozbolt and Eligehausen (1990) [1] the influence of the size of the anchor head was concluded to have small influence on the failure load. But the experimental results from Eligehausen et al. (1992) [15] and Furche (1994) [13] provided evidence for the influence of head size on the concrete cone breakout capacity. Recently this factor was also investigated experimentally by Nilforoush et al. (2018) [12]. In view of further experimental and numerical results available in literature. A more generalised comparison of the results from the present study with other results from literature is also made as shown in Fig. 8.

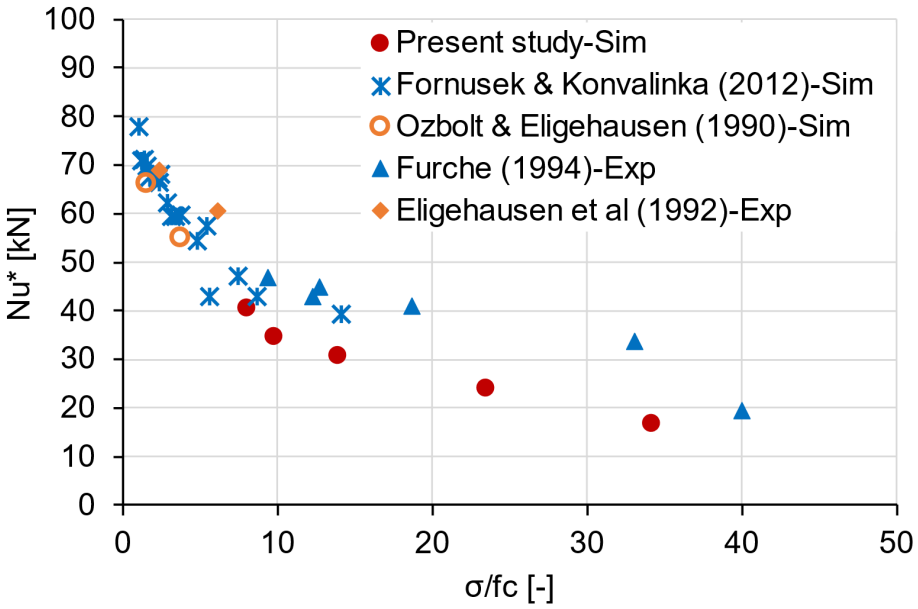

Fig. 8: Comparison between the results from the

The experimental and numerical studies referred above had tested/simulated headed studs with embedment depths between 50 mm and 500 mm and different compressive strengths. Hence, to be able to compare results from different sources the failure loads are scaled to an embedment depth of 80 mm and compressive strength of 25 MPa by multiplying the reported failure loads with $(80/h_{ef})^{1.5} \cdot (25/f_c)^{0.5}$. Since, this scaling of failure loads for higher embedment leads to a smaller ratio of bearing pressure to compressive strength (σ/25), results

only for embedment depth from 75 mm to 150 mm are used for the comparison shown in Fig. 8. The summary of the results used for the comparison is given in Table 6.

Table 6: Summary of the experimental and numerical results

Reference	Result Type	h_{ef}	d_s	d_h	f_c[1]	N_u[2]	N_u*	σ/f_c*
[-]	[-]	[mm]			[MPa]	[kN]		[-]
Eligehausen et al. (1992)# [15]	Exp	150	24	32.9	26.52	160	60.51	6.09
		150	24	45.6	26.52	182.4	68.98	2.34
Furche (1994)# [13]	Exp	76.25	12	13	24.40	18.1	19.64	40.00
		78.50	12	14	24.40	32.4	33.72	33.02
		78.75	12	16	24.40	39.5	40.94	18.62
		77.75	12	18	24.40	42.5	44.90	12.71
		81.25	12	18	28.39	47.1	43.16	12.21
		78.67	12	20	24.40	45.3	47.03	9.36
Ozbolt & Eligehausen (1990) [1]	Sim	130	22	35	17.6	95.5	54.95	3.78
		130	22	52	17.6	115.0	66.17	1.52
Fornusek & Konvalinka (2012) [16]	Sim	90	13.5	18	25.5	47.4	39.33	14.13
		90	13.5	22.5	25.5	56.8	47.13	7.41
		90	13.5	27	25.5	69.5	57.67	5.37
		90	13.5	31.5	25.5	72.1	59.83	3.76
		90	13.5	36	25.5	75.1	62.32	2.85
		90	13.5	40.5	25.5	80.3	66.63	2.33
		120	18	24	25.5	79.7	42.96	8.68
		120	18	30	25.5	101.3	54.60	4.83
		120	18	36	25.5	110.4	59.50	3.12
		120	18	42	25.5	126.3	68.07	2.41
		120	18	48	25.5	125.7	67.75	1.74
		120	18	54	25.5	132.2	71.25	1.40
		150	22.5	30	25.5	111.6	43.04	5.57
		150	22.5	37.5	25.5	154.6	59.62	3.37
		150	22.5	45	25.5	174.4	67.26	2.26
		150	22.5	52.5	25.5	181.2	69.88	1.58
		150	22.5	60	25.5	184.3	71.08	1.17
Present study	Sim	80	12	13	25.83	17.1	16.79	34.21
		80	12	14	25.83	24.3	23.96	23.46
		80	12	16	25.83	31.2	30.67	13.95
		80	12	18	25.83	35.2	34.61	9.79
		80	12	20	25.83	41.2	40.54	8.07

#→Mean results from the test series for different embedment depths.

1→For experimental results the reported cube strengths converted to cylinder (Ø=150 mm, H=300 mm) compressive strengths and for the simulation results the compressive strength used for the simulations.

2→Average failure load for the experimental results and the predicted failure load for the simulation results.

N_u*→ $N_u \cdot \left(\frac{80}{hef}\right)^{1.5} \cdot \sqrt{\left(\frac{25}{fc}\right)}$ (Failure loaded normalised to 80 mm embedment depth and 25 MPa cylinder concrete compressive strength).

σ/f_c*→Bearing stress on the head divided by 25 MPa

5. CONLUSIONS AND OUTLOOK

Based on the validation presented in this paper it can be concluded that the Drucker-Prager concrete model with Rankine's yield surface in combination with the linear SOLID185-element in ANSYS® is able to reproduce the behaviour of headed studs away from the edge.

The influence of the head size predicted in the present study also agrees with the experimental and other numerical results available in literature. Thus, validating the model. Although, the predicted ultimate loads in the presented study were slightly lower than the respective experimental peak load. But it should be noted that the material properties for concrete were taken from Eurocode 2 and no attempt was made by the authors to calibrating the material properties or the material model input parameters to improve the comparison. Most importantly the predicted influence of the investigated parameter is correctly reproduced in the presented simulations.

In the next steps, further numerical investigations are planned to validation the model's capabilities to reproduce the response of headed studs, a) close to the edge (effect of edge distance and blow-out failure) and b) in cracked concrete.

REFERENCES

[1] OZBOLT, J., ELIGEHAUSEN, R.: *Numerical analysis of headed studs embedded in large plain concrete blocks*, In: Proceedings of second International conference on Computer aided analysis and design of concrete structures, Zell am See, Austria: Pineridge Press, Swansea UK, 1990

[2] PUKL, R., ELIGEHAUSEN, R., CERVENKA, V.: *Computer simulation of pullout tests of headed anchors in a state of plane-stress*, In: ACI SP-134, p. 79–100, 1992

[3] LAKHANI, H., HOFMANN, J., BAL, A.: *FE analysis of fasteners exposed to fire - Evaluation of concrete cone capacity*, In: Proceedings of 7th International Conference on Application of Structural Fire Engineering, Ljubljana, Slovenia, p. 192–197, 2021

[4] LAKHANI, H., HOFMANN, J.: *Concrete cone failure of headed stud under different fire exposure*, Otto-Graf-Journal, 20, p. 135–146, 2021

[5] BAŽANT, Z.P., GETTU, R., KAZEMI, M.T.: *Identification of nonlinear fracture properties from size effect tests and structural analysis based on geometry-dependent R-curves*, International Journal of Rock Mechanics and Mining Sciences & Geomechanics Abstracts, 28(1), p. 43–51, 1991

[6] BAZANT, Z.P., OZBOLT, J., ELIGEHAUSEN, R.: *Fracture size effect: review of evidence for concrete structures*, Journal of Structural Engineering, 120(8), p. 2377–2398, 1994

[7] ELIGEHAUSEN, R., SAWADE, G.: *Verhalten von Beton auf Zug. [Teil 1]*, Betonwerk + Fertigteil-Technik, 51(5), p. 315–22, 1985

[8] BAŽANT, Z.P., OH, B.H.: *Crack band theory for fracture of concrete*, Mat Constr, 16(3), p. 155–177, 1983

[9] JIRÁSEK, M., BAUER, M.: *Numerical aspects of the crack band approach*, Computers & Structures, 110–111, p. 60–78, 2012

[10] ČERVENKA, J., ČERVENKA, V., LASERNA, S.: *On crack band model in finite element analysis of concrete fracture in engineering practice*, Engineering Fracture Mechanics, 197, p. 27–47, 2018

[11] OŽBOLT, J., ELIGEHAUSEN, R., PERIŠKIĆ, G., MAYER, U.: *3D FE analysis of anchor bolts with large embedment depths, Engineering Fracture Mechanics*, 74(1–2), p. 168–178, 2007

[12] NILFOROUSH, R., NILSSON, M., ELFGREN, L.: *Experimental Evaluation of Influence of Member Thickness, Anchor-Head Size, and Orthogonal Surface Reinforcement on the Tensile Capacity of Headed Anchors in Uncracked Concrete*, Journal of Structural Engineering, 144(4), 2018

[13] FURCHE, J.: *Zum Trag- und Verschiebungsverhalten von Kopfbolzen bei zentrischem Zug* [PhD Thesis], University of Stuttgart, Institute of Construction Materials, Stuttgart, Germany, 1994

[14] ANSYS®, 2022R2: *Ansys® Academic Research Mechanical*, Release 2022 R2, 2022

[15] ELIGEHAUSEN, R., BOUSKA, P., CERVENKA, V., PUKL, R.: *Size effect of the concrete cone failure load of anchor bolts*, In: Proceedings of the First International Conference on Fracture Mechanics of Concrete Structures, Breckenridge, Colorado, USA: CRC Press, 1992

[16] FORNŮSEK, J., KONVALINKA, P.: *Numerical investigation of head diameter influence on tensile capacity of headed studs*, In: 2012 IEEE Symposium on Business, Engineering and Industrial Applications, p. 737–741, 2012

[17] ANSYS DOCUMENTATION: *Mechanical APDL Element Reference, Chapter 7 Element Library*, (ANSYS Help, 2022R2)

[18] LAKHANI, H., HOFMANN, J.: *Numerical studies on the effect of spalling on the concrete cone capacity of single headed stud during fire*, In: Proceedings of the 7th International Workshop on Concrete Spalling due to Fire Exposure, Berlin, Germany: Bundesanstalt für Materialforschung und -prüfung (BAM), p. 153–163, 2022

[19] ANSYS DOCUMENTATION: *Mechanical APDL Material Reference, Chapter 4.10.5 Drucker-Prager Concrete*, (ANSYS Help, 2022R2)

[20] EN1992-1-1:2004: *Eurocode 2: Design of concrete structures - Part 1-1: General rules and rules for buildings*, Brussels: European Committee for standardization, 2004

[21] LOCH, M.: *Beitrag zur Bestimmung von charakteristischen Werkstofffestigkeiten in Bestandstragwerken aus Stahlbeton* [PhD Thesis], Technical University of Kaiserslautern, Kaiserslautern, Germany, 2014